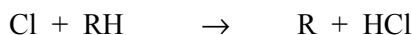


$= 3 \times 10^{16}$ atoms cm^{-3} .⁵ Thus, photolysis of oxalyl chloride provides a "clean" photolytic source of Cl atoms (in the sense that no other reactive species are formed in the photolysis process in any appreciable amounts).^{3,4} Cl atoms formed were immediately converted into R radicals by reaction with RH:



RH concentrations were in large excess over those of chlorine atoms and sufficient to ensure the complete conversion of Cl atoms to the R radicals. Thus, no active species other than R were present in the system during the kinetics of R decay. Initial concentrations of the radicals studied were determined using the measured (in real time) production of HCl or photolytic depletion of oxalyl chloride. The kinetics of R decay was monitored in real time and the values of the rate constant of the R + R self-reactions were determined from the R temporal profiles.

The rate constant of reaction 1 ($\text{C}_2\text{H}_5 + \text{C}_2\text{H}_5$)⁶ was found to decrease with temperature from $2.7 \times 10^{-11} \text{cm}^3 \text{molecule}^{-1} \text{s}^{-1}$ at room temperature to $1.6 \times 10^{-11} \text{cm}^3 \text{molecule}^{-1} \text{s}^{-1}$ at 800K. The temperature dependence of the rate constant can be described by the following expression:

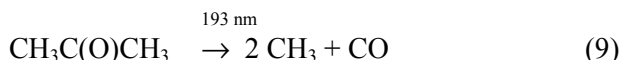
$$k_1 = 5.45 \times 10^{-5} \text{T}^{-2.106} \exp(-756 \text{K/T}) \text{cm}^3 \text{molecule}^{-1} \text{s}^{-1}$$

Both C_2H_4 and C_4H_{10} were observed as primary products of reaction 1, indicating the importance of both the recombination and the disproportionation channels under the experimental conditions.

The rate constant of reaction 2 ($\text{C}_3\text{H}_3 + \text{C}_3\text{H}_3$)⁷ decreased with temperature from $3.3 \times 10^{-11} \text{cm}^3 \text{molecule}^{-1} \text{s}^{-1}$ at 500 K to $2.8 \times 10^{-11} \text{cm}^3 \text{molecule}^{-1} \text{s}^{-1}$ at 700K and $1.3 \times 10^{-11} \text{cm}^3 \text{molecule}^{-1} \text{s}^{-1}$ at 1000K. The low value at 1000 K is likely to be due to the falloff effects. Products of reaction 2 were studied in real-time experiments as well as by GC/MS analysis, which demonstrated dependence of the distribution of products of reaction 2 on temperature.

2. R + CH₃ cross-combination reactions.

The R + CH₃ rate constant measurements (R = C_3H_5 , C_3H_3 , C_2H_5 , *n*- C_3H_7 , *n*- C_4H_9 , and CCl_3) were performed⁸⁻¹⁰ under pseudo-first-order conditions using a method similar to that used earlier by Niiranen and Gutman.¹¹ CH₃ and R radicals were produced by the 193-nm photolysis of acetone



and the simultaneous photolysis of the precursor of the R radicals. Under the experimental conditions used in the current work, reaction 9 accounts for more than 95 % of acetone photolysis.¹² Concentrations of radical precursors were selected to create a large excess of initial concentrations of methyl radicals over the total combined concentration of all the remaining radicals formed in the system, so that the R + CH₃ process under study dominates all other minor reactions of R. Under these conditions, the recombination of methyl radicals



was essentially unperturbed by the presence of the other radicals. At the same time the kinetics of R decay was completely determined by the reaction with CH₃ and practically unaffected by the self-recombination reaction and by reactions with other active species formed in the system. Heterogeneous loss was the only additional sink of methyl and R radicals that had to be taken into account. The temporal evolution of the ion signals of R, CH₃, and $\text{CH}_3\text{C}(\text{O})\text{CH}_3$ was monitored in real time. Initial concentrations of CH₃ were obtained from the photolytic depletion of acetone. Typical temporal radical signal profiles are presented in Figure 1. Under each set of conditions, the values of the rate constant of reaction 1 were obtained from the observed radical decay profiles.

Corrections for the falloff effects had to be applied to the experimental values of the rate constants of reactions 3 – 5. These corrections were calculated using the Master Equation approach. Reactions 6 – 8 are in the high-pressure limit under the experimental conditions used. The resultant

temperature dependences of the high-pressure-limit rate constants of reactions 3 – 8 can be represented by the following expressions (units are $\text{cm}^3 \text{ molecule}^{-1} \text{ s}^{-1}$):

$$\begin{aligned} k_3^\infty &= 1.55 \times 10^{-9} T^{-0.54} \exp(117 \text{ K}/T) & k_4^\infty &= 6.80 \times 10^{-11} \exp(130 \text{ K}/T) \\ k_5^\infty &= 2.36 \times 10^{-11} \exp(433 \text{ K}/T) & k_6^\infty &= 3.06 \times 10^{-11} \exp(387 \text{ K}/T) \\ k_7^\infty &= 2.28 \times 10^{-11} \exp(473 \text{ K}/T) & k_8^\infty &= 2.04 \times 10^{-11} \end{aligned}$$

Discussion. “Geometric mean rule.”

In spite of the importance of the radical-radical cross-combination reactions in the mechanisms of combustion and pyrolysis of hydrocarbon fuels, reliable rate and branching data on this type of reaction are sparse as these reactions are difficult to study experimentally because of the high reactivity of the chemical species involved. Due to the lack of directly obtained experimental values, rate are often estimated using the “geometric mean rule”.¹³⁻¹⁵

$$k_{AB} = 2(k_{AA}k_{BB})^{1/2} \quad (\text{I})$$

Here k_{AB} is the rate constant of the A + B reaction and k_{AA} and k_{BB} are the rate constants of the A + A and B + B self-reactions, respectively. Validation of the geometric mean rule, however, is also problematic for the same reason, i.e., a deficit of directly obtained experimental rate constant values.

The newly available experimental rate data obtained in direct experiments provide an opportunity for evaluation of the validity of the “geometric mean rule.” Figures 2 – 6 present the experimental data on the temperature dependences of the rate constants of reactions 3 – 6 and 8 together with the results of evaluation of these rate constants via formula I.

Use of expression I requires knowledge of k_{AA} and k_{BB} , the rate constants of the A + A and B + B self-reactions. The rate constants of methyl radical self-reaction (reaction 10) are well known. In the calculations according to the “geometric mean rule,” we used the parameterization of Hessler and Ogren¹⁶ ($k_8^\infty(298 \text{ K}) = 5.81 \times 10^{-11} \text{ cm}^3 \text{ molecule}^{-1} \text{ s}^{-1}$) with 20% uncertainty. The values of C_2H_5 and C_3H_3 self-reactions rates used here are from the experimental studies described in this work,^{6,7} except for the room-temperature value of k_2 , which was obtained from the studies of refs 17 and 18. Data on the C_3H_5 and CCl_3 self-reactions were obtained from direct temperature-dependent studies of refs 19 and 20. The room-temperature rate constant of the self-reaction of $n\text{-C}_3\text{H}_7$ radicals was obtained from ref 21.

As can be seen from the plots in Figures 2 – 6, the values of the R + CH_3 reaction rate constants calculated using the “geometric mean rule” are in reasonable agreement with the experimental values. The only significant deviation from experiment is observed for reaction 6, that of $n\text{-C}_3\text{H}_7$ with CH_3 . This disagreement between the experimental and calculated values of k_6 may lead to the conclusion of inadequacy of the “geometrical mean rule”; however, one should keep in mind that this conclusion would critically depend on the accuracy of the rate constant value used for the n -propyl radical self-reaction, which is the result of only one room-temperature measurement performed by one group.²¹ At the same time, the agreement observed for reactions 3, 4, 5, and 8 provide support to the “geometric mean rule.”

Acknowledgement

This research was supported by Division of Chemical Sciences, Office of Basic Energy Sciences, Office of Energy Research, U.S. Department of Energy under Grant No. DE/FG02-94ER14463 and, in part, by the U.S. National Science Foundation, Combustion and Thermal Plasmas Program under Grant No. CTS-0105239.

Figure captions

Figure 1. Examples of temporal ion signal profiles obtained in the experiments to measure the rate constants of the $\text{CCl}_3 + \text{CH}_3$ reaction. $T = 800 \text{ K}$, $[\text{He}] = 1.20 \times 10^{17}$, $[\text{CCl}_3\text{C}(\text{O})\text{CCl}_3] = 4.6 \times 10^{11}$, $[\text{CH}_3\text{C}(\text{O})\text{CH}_3] = 3.35 \times 10^{13}$, $[\text{CCl}_3]_0 \leq 8.8 \times 10^{10}$, $[\text{CH}_3]_0 = 5.82 \times 10^{12} \text{ molecule cm}^{-3}$.

Figure 2. Temperature dependences of the experimentally obtained values of the rate constant of the $C_3H_5 + CH_3$ reaction, k_3 , (filled circles) and extrapolated values of k_3^∞ (open smaller circles). Square represents the k_3 value reported by Garland and Bayes.¹⁵ Solid and dashed lines are the central and the limiting values of k_3^∞ calculated using the “geometric mean rule.”

Figure 3. Temperature dependences of the experimentally obtained values of the rate constant of the $C_3H_3 + CH_3$ reaction, k_4 , (filled circles) and extrapolated values of k_4^∞ (open smaller circles). Square represents the k_4 value reported by Fahr and Nayak.¹⁷ Solid and dashed lines are the central and the limiting values of k_4^∞ calculated using the “geometric mean rule.”

Figure 4. Temperature dependences of the experimentally obtained values of the rate constant of the $C_2H_5 + CH_3$ reaction, k_5 (filled circles) and extrapolated values of k_5^∞ (open smaller circles). Filled square, open square, and triangle represent the room-temperature k_5 values reported by Anastasi and Arthur²², Garland and Bayes¹⁵, and Sillesen et al.,²³ respectively. Solid and dashed lines are the central and the limiting values of k_5^∞ calculated using the “geometric mean rule.”

Figure 5. Temperature dependences of the experimentally obtained values of the rate constant of the $n-C_3H_7 + CH_3$ reaction, k_6 (filled circles) and extrapolated values of k_6^∞ (open smaller circles). Near coincidence of the filled and the open circles (open small circles are superimposed on the larger filled circles) demonstrates that reaction 6 is at the high pressure limit under the conditions of all experiments. Shaded area demonstrates the uncertainty ranges of k_6^∞ calculated using the “geometric mean rule” and the room-temperature value of the rate constants of the $n-C_3H_7 + n-C_3H_7$ reaction reported by Adachi and Basco.²¹

Figure 6. Temperature dependences of the experimentally obtained values of the rate constant of the $CCl_3 + CH_3$ reaction, k_8 (circles). Solid and dashed lines are the central and the limiting values of k_8 calculated using the “geometric mean rule.”

References

1. Slagle, I. R.; Gutman, D. *J. Am. Chem. Soc.* **1985**, *107*, 5342.
2. Stoliarov, S. I.; Knyazev, V. D.; Slagle, I. R. *J. Phys. Chem. A* **2000**, *104*, 9687.
3. Baklanov, A. V.; Krasnoperov, L. N. *J. Phys. Chem. A* **2001**, *105*, 97.
4. Baklanov, A. V.; Krasnoperov, L. N. *J. Phys. Chem. A* **2001**, *105*, 4917.
5. Nicovich, J. M.; Kreutter, K. D.; Wine, P. H. *J. Chem. Phys.* **1990**, *92*, 3539.
6. Shafir, E. V.; Slagle, I. R.; Knyazev, V. D. *Manuscript in preparation*.
7. Shafir, E. V.; Slagle, I. R.; Knyazev, V. D. *Manuscript in preparation*.
8. Knyazev, V. D.; Slagle, I. R. *J. Phys. Chem. A* **2001**, *105*, 3196.
9. Knyazev, V. D.; Slagle, I. R. *J. Phys. Chem. A* **2001**, *105*, 6490-6498.
10. Knyazev, V. D.; Slagle, I. R.; Bryukov, M. G. *Manuscript in preparation*.
11. Niiranen, J. T.; Gutman, D. *J. Phys. Chem.* **1993**, *97*, 9392.
12. Lightfoot, P. D.; Kirwan, S. P.; Pilling, M. J. *J. Phys. Chem.* **1988**, *92*, 4938.
13. Kerr, J. A.; Trotman-Dickenson, A. F. *Prog. React. Kinet.* **1961**, *1*, 105.
14. Blake, A. R.; Henderson, J. F.; Kutschke, K. O. *Can. J. Chem.* **1961**, *39*, 1920.
15. Garland, L. J.; Bayes, K. D. *Journal of Physical Chemistry* **1990**, *94*, 4941.
16. Hessler, J. P.; Ogren, P. J. *J. Phys. Chem.* **1996**, *100*, 984.
17. Fahr, A.; Nayak, A. *International Journal of Chemical Kinetics* **2000**, *32*, 118.
18. Atkinson, D. B.; Hudgens, J. W. *J. Phys. Chem. A* **1999**, *103*, 4242.
19. Tulloch, J. M.; Macpherson, M. T.; Morgan, C. A.; Pilling, M. J. *J. Phys. Chem.* **1982**, *86*, 3812.
20. Danis, F.; Caralp, F.; Veyret, B.; Loirat, H.; Lesclaux, R. *Int. J. Chem. Kinet.* **1989**, *21*, 715.
21. Adachi, H.; Basco, N. *Int. J. Chem. Kinet.* **1981**, *13*, 367.
22. Anastasi, C.; Arthur, N. L. *J. Chem. Soc. Faraday Trans. 2* **1987**, *83*, 277.
23. Sillesen, A.; Ratajczak, E.; Pagsberg, P. *Chem. Phys. Lett.* **1993**, *201*, 171.

